ELSEVIER

Journal of Electroanalytical Chemistry 527 (2002) 71–84

Journal of Electroanalytical Chemistry

www.elsevier.com/locate/jelechem

Electrochemical impedance spectroscopy of thiourea electro-oxidation on copper electrodes in aqueous 0.5 M sulphuric acid

L.M. Gassa, J.N. Lambi [1], A.E. Bolzán *, A.J. Arvia

Facultad de Ciencias Exactas, Instituto de Investigaciones Fisicoquímicas Teóricas y Aplicadas, INIFTA, Universidad Nacional de la Plata, UNLP, CONICET, Sucursal 4, Casilla de Correo 16, 1900 La Plata, Argentina

Received 22 December 2001; received in revised form 5 March 2002; accepted 5 March 2002

Abstract

The anodisation of copper electrodes in aqueous thiourea (TU) containing 0.5 M sulphuric acid is studied by electrochemical impedance spectroscopy (EIS) combined with rotating disk electrode and ring-disk electrode, SEM and EDAX techniques. For $E < -0.35$ V (vs. MSE), Nyquist plots show two time constants. The first one, which appears at high frequencies, involves the contribution of the double layer capacity and the charge transfer resistance related to the electro-oxidation of TU to formamidine disulphide (FDS). The second time constant, which is observed at low frequencies, is related to complex electrochemical and chemical processes following TU electro-oxidation to FDS. Depending on the applied potential, this time constant can be assigned to either an electroadsorption process from TU electro-oxidation products or an electrochemical process under diffusion through an anodic film. At high TU concentration, the low frequency time constant corresponds to the typical response of a pure capacitor due to the formation of a thick anodic film under a diffusion controlled process. In this case, for $E \geq -0.35$ V, Nyquist plots exhibit at least three time constants and an inductive loop. The inductive loop is due to surface relaxation associated with copper pitting. The formation of different types of anodic films is confirmed by SEM observations. EIS results are consistent with the complex reaction pathway previously proposed for the anodisation of copper in aqueous TU-containing acid solutions.

Keywords: Thiourea; Copper; Electrochemical impedance spectroscopy; Electro-oxidation; Anodic films

1. Introduction

The study of electrochemical processes on metals involving solution constituents that are used as additives for corrosion inhibition is of importance from both theoretical and practical points of view. It provides information to establish the nature of possible intermediate compounds involved in these processes, and to understand corrosion inhibition and protection mechanisms. In this respect, thiourea (TU), a relatively simple molecule that interacts with a number of metal surfaces such as copper [1], iron [2], gold [3] and silver [4], is of practical interest as an additive and appears to be suitable as a model system for the metal additive solution interface [5–7].

The behaviour of copper in aqueous environments containing TU becomes relatively complex due to the concurrence of electrochemical reactions at the Cu | TU-containing solution interface [1,8], chemical reactions between TU and copper ions in solution [9] and strong chemisorption of TU and its reaction products [10]. The extent of copper surface coverage by TU at the open circuit potential (E_{oc}) is comparable to that of gold and silver, as was recently confirmed from the underpotential deposition of thallium as a test reaction [11] and scanning tunnelling microscopy (STM) imaging [12,13].

Formamidine disulphide, $(H_2N)_2(HN)_2C_2S_2$, (FDS) is the first electro-oxidation product from TU that is produced at potentials lower than the threshold potential for copper electrodissolution [1]. It can also be produced by a homogeneous electrochemical reaction

* Corresponding author. Fax: +54-221-4254642.
E-mail address: aebolzan@inifta.unlp.edu.ar (A.E. Bolzán).
[1] On leave from Ecole Normale Supérieure, University of Yaounde I, Cameroon.

0022-0728/02/$ - see front matter
PII: S0022-0728(02)00829-X

between TU and Cu(II) ions [8], yielding a number of different Cu(I)–TU complex ions in solution of the formula $[Cu_x(TU)_y]^{x+}$. Recently [14], complex Cu(I)–TU salts with cation stoichiometry such as $[Cu_2(TU)_5]^{2+}$ (complex I), $[Cu_4(TU)_7]^{4+}$ (complex II) and $[Cu_2(TU)_6]^{2+}$ (complex III) have been crystallised from either the anodisation of copper in aqueous TU-containing 0.5 M sulphuric acid or simply by chemical reaction of dissolved TU and aqueous acid copper sulphate. In contrast to soluble complexes I and III, insoluble complex II is formed as a polymer-like solid for a Cu(II)/TU molar ratio close to 4/7. The formation of a copper–TU–sulphate complex film in the potential range related to copper electrodissolution has recently been confirmed from quartz crystal microbalance measurements [15]. Furthermore, TU may undergo polycondensation to polythiourets in acids [10]. It has also been shown that FDS is capable of Cu(I) ion complexation [8].

The electro-oxidation of copper in either aqueous TU- or FDS-containing sulphuric acid solutions, at 298 K, in the range $-0.70 \leq E \leq -0.34$ V (mercurous sulphate electrode (MSE)) and concentrations of TU (c_{TU}) lower than a certain critical value, $c_{TU} < c_{TU,c} \cong 2.5$ mM), yields FDS and soluble Cu(I) ionic complex species as the main products [11]. For $c_{TU} \simeq c_{TU,c}$ and low E, the insoluble Cu(I)–TU complex film passivates copper, whereas for $c_{TU} > c_{TU,c}$ its dissolution to soluble copper complexes is favoured. The Faradaic yield of these reactions and the nature of both the soluble products and passivating film depend on the applied potential, Cu(II)/TU concentration ratio and the type of anion present in the solution [14,16–18].

The kinetics of Cu | TU-containing anodic film formation has also been studied by following the evolution of the copper corroding front by on line in situ imaging [19]. For $E < -0.34$ V, film (I) is formed first and its growth kinetics fit a parabolic law resulting from the slow diffusion of either TU from the solution to the copper surface or Cu(I) ions in the reverse direction. The latter process also involves copper sludge formation.

At the standard copper electrode potential (E^0_r(Cu(0)/Cu(II) = −0.31 V vs. MSE) at 298 K) besides copper electro-oxidation to Cu(I) and Cu(II), the electro-oxidation of TU and FDS takes place to produce NH_4^+, CO_2, sulphuric acid and surface residues. The yield of each one of these reactions depends on the experimental conditions [20].

For $E > -0.34$ V, the electrodissolution of copper as Cu(II) takes place in the presence of a heterogeneous film resulting from the electrochemical oxidation of TU and FDS-derivatives formed at low potentials. In this case, the main reactions are the electrodecomposition of both FDS and Cu(I)–TU complexes yielding a copper sulphide-containing film (film II), and the electrodissolution of copper to aqueous Cu(II) ions in TU depleted solutions through film II. The growth kinetics of film II approach a linear film thickness versus anodisation time relationship [19]. The rate of this process appears to be governed by a surface electrochemical reaction on copper. Film II consists mainly of either Cu_2S or a mixture of CuS and Cu, as concluded from XPS [11], and its rupture assists the localised corrosion of copper.

Therefore, the broad picture of the electrochemistry of Cu in TU-containing solutions shows that there are a number of questions still open for research, in particular, those issues related to the influence of the various films on the corresponding electrochemical kinetics, the electrical behaviour of the anodic films and the equivalent circuits accounting for a reasonable description of the electrochemical interface when either homogeneous copper electrodissolution conditions are approached or localised corrosion dominates the global anodic process.

The aim of this work is to investigate the dynamics of the electrochemical interface during the anodisation of copper in TU-containing 0.5 M sulphuric acid covering the potential range from the rest potential to the copper electrodissolution potential, combining electrochemical impedance spectroscopy (EIS), voltammetry, SEM and EDAX surface analysis techniques. This work provides further data on the electrochemical oxidation of TU and the formation of different anodic films during the passivation of copper which are consistent with the reaction pathways that were advanced in previous publications [11,19,21].

2. Experimental

The experiments were performed using a conventional glass-made three-electrode cell utilising electrorefined polycrystalline copper wires (diameter 0.5 mm, geometric area ca. 0.6 cm^2) as working electrodes (WE). Each WE was polished mechanically using alumina–water suspension and washed thoroughly with water before each experiment. The counter electrode (CE) was a large platinum sheet (2 cm^2 apparent area) and the reference electrode (RE) was a MSE, its scale shifted by 0.65 V with respect to the SHE scale. The working solution was freshly prepared aqueous x M TU ($10^{-4} \leq x \leq 0.5$) + 0.5 M sulphuric acid prepared from TU (Fluka, puriss. p.a.), sulphuric acid (97% Merck, p.a.) and Milli-Q* water. It was kept under nitrogen saturation before and during the experiment.

Electrochemical impedance measurements were carried out using a Zahner IM6d potentiostat with a frequency analyser. The experiments were performed applying a sine waveform perturbation with amplitude 5×10^{-3} V, while scanning the modulus of impedance and the phase shift in the frequency range $10^{-3} \leq f \leq 10^5$ Hz, and the applied potential in the range $-0.90 \leq E \leq -0.3$ V.

Complementary voltammetric, rotating disk (RDE) and rotating ring-disk (RRDE) techniques were also utilised. The formers were performed using a conventional electrochemical setup consisting of a conventional potentiostat with a wave generator coupled to a Houston Omnigraphic recorder. RDE and RRDE runs were carried out using either a rotating copper disk (type ED 10K Taccussel) or a rotating copper-disk/platinum-ring electrode (type EAD 10K Tacussel, geometric area 0.12 cm^2, collection efficiency $N = 0.24$). Both RRDE and RDE experiments were performed using a type BI-PAD Tacussel bipotentiostat.

SEM micrographs and EDAX analysis of anodised copper electrodes were obtained using model XL30 FEG Philips equipment.

Potentials in the text are given on the MSE scale. Runs were made at 298 K.

3. Results

3.1. Voltammetric data

A typical cyclic voltammogram (blank) of copper in aqueous 0.5 M sulphuric acid run at $v = 0.05$ V s^{-1} (Fig. 1) from −0.8 to −0.38 V exhibits a small cathodic current contribution up to approximately −0.75 V due to the electrodeposition of copper that was electrodissolved in previous cycles, and an anodic current that increases from −0.75 V upwards, mainly due to the $Cu(0) = Cu(II) + 2e^-$ overall reaction [21]. The subsequent negative potential scan shows a decreasing anodic current that reaches null current at −0.42 V, followed by a broad asymmetric cathodic peak at approximately −0.5 V due to the electrodeposition of Cu(II) ions formed in the preceding scan. This process contributes to the cathodic current plateau that extends from about −0.6 to −0.8 V and from −0.8 to −0.42 V.

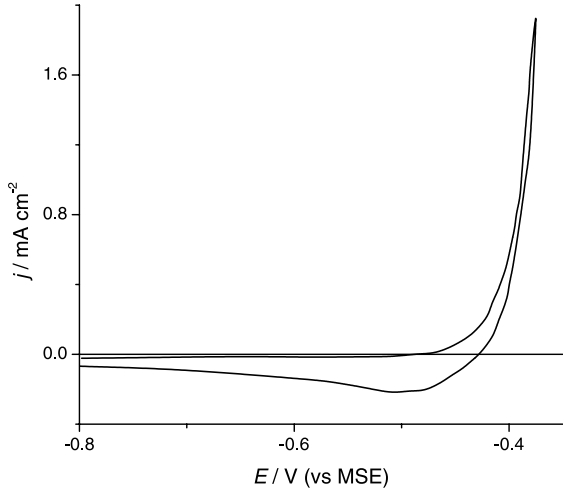

Fig. 1. Cyclic voltammogram for copper in aqueous 0.5 sulphuric acid. $v = 0.05$ V s^{-1}, 298 K.

Comparable cyclic voltammograms of copper in aqueous TU-containing 0.5 M sulphuric acid (Fig. 2) show the following features. For $c_{TU} = 0.1$ mM the positive potential scan exhibits an anodic current from −0.9 V upwards with humps Ia at approximately −0.53 V related to the electro-oxidation of TU to FDS [21]. Then, the anodic current increases abruptly due to passivity breakdown and the electrodissolution of copper to Cu(II) aqueous ions. The subsequent reverse potential scan shows a small peak IIc at approximately −0.49 V assigned to the electroreduction of Cu(II) ions to Cu(0) and peak Ic assigned to the electroreduction of FDS to TU [21]. Peak IIIc, appearing at approximately −0.8 V is tentatively assigned to Cu(I)–TU complexes electroreduction.

For $c_{TU} = 1$ mM (Fig. 2b), the above voltammetric features change markedly. The positive potential scan shows a net current peak Ia at −0.62 V and a hump IIa at −0.45 V. The reverse scan exhibits peak IIc related to the electroreduction of Cu(I) complexes, and peak Ic at approximately −0.8 V as in Fig. 2a. The conjugated pair of peaks Ia/Ic is related to the $TU \rightleftharpoons FDS + 2H^+ + 2e^-$

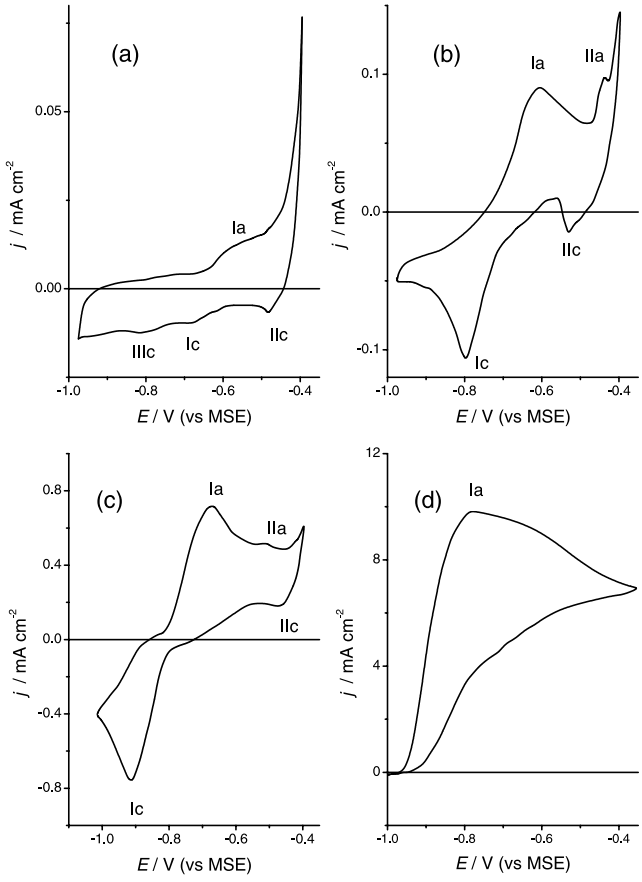

Fig. 2. Cyclic voltammograms for copper in aqueous x mM TU + 0.5 M sulphuric acid, (a) $x = 0.1$; (b) $x = 1$; (c) $x = 10$; (d) $x = 500$. $v = 0.05$ V s^{-1}, 298 K.

reaction [15,21]. As seen from the comparison of Figs. 1 and 2a at −0.49 V, the presence of TU produces a remarkable inhibition of copper electrodissolution.

When $c_{TU} = 10$ mM (Fig. 2c), both peaks Ia and IIa are shifted negatively. The height of both peaks Ia and Ic increases almost linearly with c_{TU} and their height ratio is close to 1.

Finally, for $c_{TU} = 0.5$ M (Fig. 2d), the anodic process starts at approximately −0.95 V resulting in a broad peak Ia at approximately −0.83 V. The reverse scan behaves as a diffusion controlled current loop, presumably involving two limiting current contributions, one associated with Cu(I)–TU complex formation at $E > -0.7$ V, and another one related to FDS electroformation in the range −1.0– −0.7 V, approximately.

The voltammograms are in agreement with previously reported data [19] that concluded that the most efficient inhibition of copper electrodissolution is obtained for $c_{TU} \simeq c_{TU,c} \simeq 2.5$ mM. For $c_{TU} > c_{TU,c}$ the contribution of TU electrochemical reactions is increased and the electrodissolution of copper, particularly by formation of Cu(I)–TU complexes at the reaction interface, is favoured.

3.2. Rotating ring-disk data

For $c_{TU} = 1$ mM rotating ring-disk voltammograms are relevant from the standpoint of the contribution of diffusion processes to the electrochemical reactions.

A typical set of current/potential curves for the disk and ring electrodes in aqueous 1 mM TU+0.5 M sulphuric acid from −1.0 to −0.35 V at $v = 0.05$ V s^{-1} and $\omega = 2000$ rpm is shown in Fig. 3a–b. The copper disk (Fig. 3a) exhibits a very small cathodic current between −1.0 and −0.8 V, an anodic current that increases to a quasi-limiting value at −0.5 V, a small hump (I_1^d) at approximately −0.42 V, and a rising anodic current for $E > -0.44$ V. The reverse potential scan shows a hysteresis loop with a minimum negative peak I_2^d at approximately −0.43 V, and a current that increases up to a maximum at approximately −0.5 V. These results indicate that in the range $-0.7 \leq E_D \leq -0.35$ V there is a mass transport of reacting species from the solution coupled with surface electrochemical reactions. The analysis of these processes for different values of c_{TU}, v and ω is reported elsewhere [21].

The simultaneous current response at the ring electrode held at $E_r = -0.9$ V (Fig. 3b) shows a cathodic current that increases steadily with the anodic current at the disk. The ring current tends to a limiting value at approximately −0.5 V, and reaches a minimum at approximately −0.42 V. The subsequent reverse scan shows first an increase in cathodic current followed by the appearance of peak I_2^r for $E_D \simeq -0.43$ V. Afterwards, the current follows a sigmoid-type function with

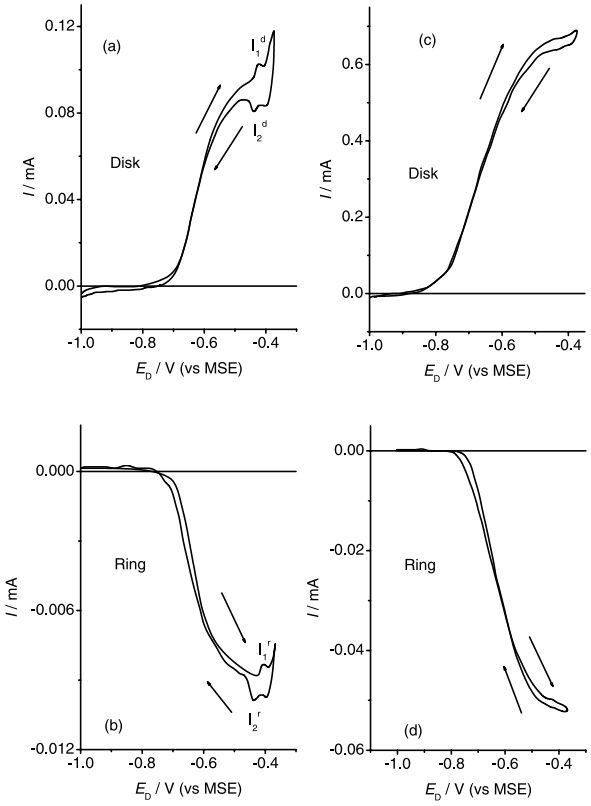

Fig. 3. Ring and disk voltammograms for copper in aqueous 1 mM TU+0.5 M sulphuric acid (a, b) and aqueous 10 mM TU+0.5 M sulphuric acid (c, d). $v = 0.05$ V s^{-1}; $\omega = 2000$ rpm; $E_r = -0.9$ V, 298 K.

E_D, as observed for the previous positive potential scan, and decreases to zero at approximately −0.73 V.

When c_{TU} is increased to 10 mM (Fig. 3c), those peaks I_1^d and I_2^d, which are found for $c_{TU} = 1$ mM, are no longer observed. The overall voltammogram displays an anodic current plateau with a small hysteresis loop. Likewise, the cathodic current at the ring (Fig. 3d) exhibits a sigmoid-type response concomitantly with the disk response. These results at intermediate c_{TU} are consistent with the formation of an insoluble anodic film on copper [11,19] that gradually inhibits copper electrodissolution competing with the solubilisation of the film as c_{TU} is further increased. In these cases, the electrodissolution of copper is also favoured by the greater concentration of TU at the reaction interface.

3.3. Impedance data

3.3.1. Stationary electrode

Impedance measurements were performed for copper electrodes immersed in both aqueous 0.5 M sulphuric acid (blank), and aqueous TU-containing 0.5 M sulphuric acid varying c_{TU} from 10^{-4} to 0.5 M under both quiescent solution and electrode rotation to indicate the

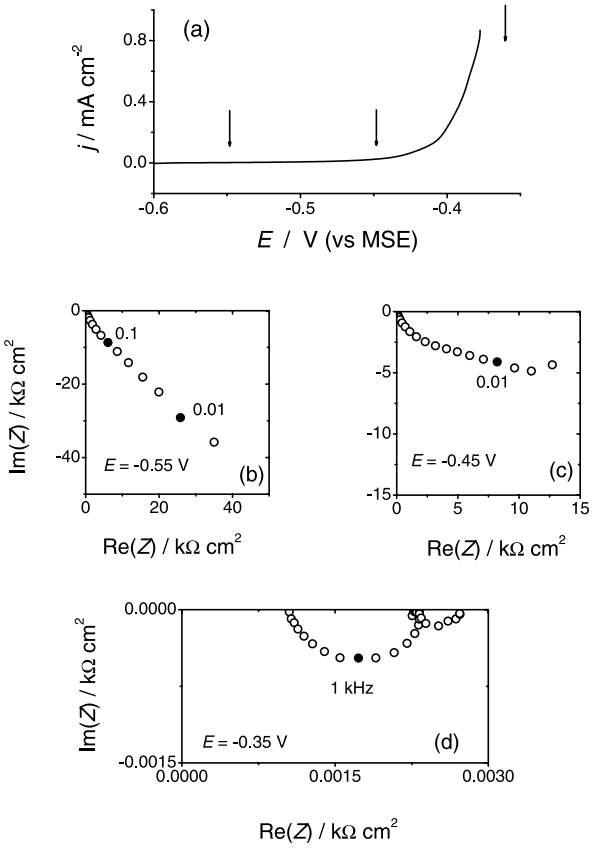

Fig. 4. Copper in aqueous 0.5 M sulphuric acid. (a) Quasi-stationary polarisation recorded at $v = 0.0005$ V s^{-1}. (b–d) Impedance spectra at different E as indicated by the arrows in (a).

participation of diffusional contributions in the electrochemical process.

For copper in aqueous 0.5 M sulphuric acid (Fig. 4), EIS at $E = -0.55$ V shows a capacitive constant at high frequencies and a Warburg behaviour at both intermediate and low frequencies (Fig. 4b). The Warburg line slowly deviates towards the real axis as the potential is shifted to -0.45 V. This behaviour (Fig. 4c) is expected for either a capacitive or time constant that is associated with a finite-length diffusion process [22]. When E is set close to E_r^0(Cu(0)/Cu(II)), two capacitive time constants at high and low frequency, respectively and an inductive contribution at intermediate frequency, are observed (Fig. 4d). In this case, the impedance values decrease drastically as compared with the former values.

For copper in aqueous 0.1 mM TU + 0.5 M sulphuric acid EIS (Fig. 5) shows characteristics similar to those corresponding to copper in aqueous 0.5 M sulphuric acid, although, in the presence of TU, the diffusion contribution extends over most of the frequency range (Fig. 5b–f). It should be noted that the Warburg contribution does not exhibit the typical 45° slope in the Nyquist plots. However, the fitting procedure of experimental data, as discussed further on, involves a value of α close to 0.5, as expected for an electrochemical process that is controlled by diffusion from the solution. For $E = -0.35$ V, the Nyquist diagram shows no inductive loop probably, because of copper corrosion inhibition by TU adsorption. At the same time, there is a drastic decrease in the values of the impedance. This means that there is an increase in the rate of the electrochemical processes taking place at this potential.

As c_{TU} is increased E_{oc} shifts negatively [21], the values of impedance decrease, and the different time constants are more clearly distinguished (Figs. 6 and 7). For aqueous 1 mM TU + 0.5 M sulphuric acid (Fig. 6) the Nyquist plot at $E = -0.69$ V, a value close to E_{oc}, shows a capacitive semicircle (Fig. 6b). As E is shifted positively, the capacitive semicircle at high frequencies is slightly distorted and the Warburg-type contribution at low frequencies (Fig. 6c) continues to be observed. Otherwise, in the range $-0.59 \leq E \leq -0.39$ V, the time constant associated with the Warburg-type impedance appears to be related to a finite-length diffusion process [23], probably due to the presence of the anodic film on copper.

On the other hand, for $c_{TU} = 10$ mM and $E \leq -0.55$ V, two time constants are observed (Fig. 7b–d), associated with a capacitive contribution at high frequencies, and the Warburg-type contribution at low frequencies. For $E > -0.55$ V, the diffusional impedance is enhanced and the approximately 45° slope straight line extends over most of the frequency range (Fig. 7e–f). Eventually, for $E \geq E_r$(Cu/Cu(II)), EIS displays two capacitive time constants and an inductive contribution at intermediate frequencies, (Fig. 7g). This is accompanied by the decrease in impedance.

For $c_{TU} = 0.5$ M (Fig. 8) EIS presents characteristics similar to those obtained for lower c_{TU}, i.e. two time constants with the capacitive loop at high frequencies and the Warburg-type contribution at low frequencies. However, for this value of c_{TU}, and at low frequencies, the diffusion impedance tends to approach a vertical line as one would expect for a finite length effect [23] (Fig. 8f). Accordingly, the corresponding polarisation curve shows an electro-oxidation process under quasi-stationary mass transport control (Fig. 8a). Eventually, for $E = -0.35$ V (Fig. 8g), the Nyquist plot shows a non-completed capacitive loop at low frequencies.

3.3.2. Rotating disk electrode

Considering that diffusion of reacting species appears to contribute to the EIS response of the copper electrode in TU-containing solutions, the influence of hydrodynamic conditions on EIS was studied by rotating a copper disk electrode at $\omega = 2000$ rpm in 1 mM TU + 0.5 M sulphuric acid (Fig. 9). These measurements allow us to establish undoubtedly that the linear behaviour observed in the Nyquist plots for copper in 1 mM TU + 0.5 M sulphuric acid, though not exhibiting the theore-

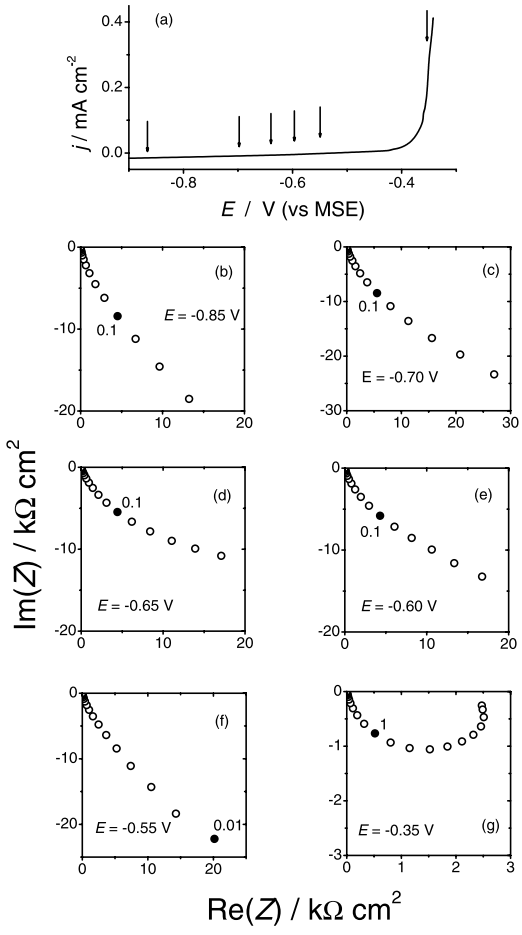

Fig. 5. Copper in aqueous 0.1 mM TU+0.5 M sulphuric acid. (a) Quasi-stationary polarisation curve recorded at $v = 0.0005$ V s^{-1}. (b–g) Impedance spectra at different E as indicated by the arrows in (a).

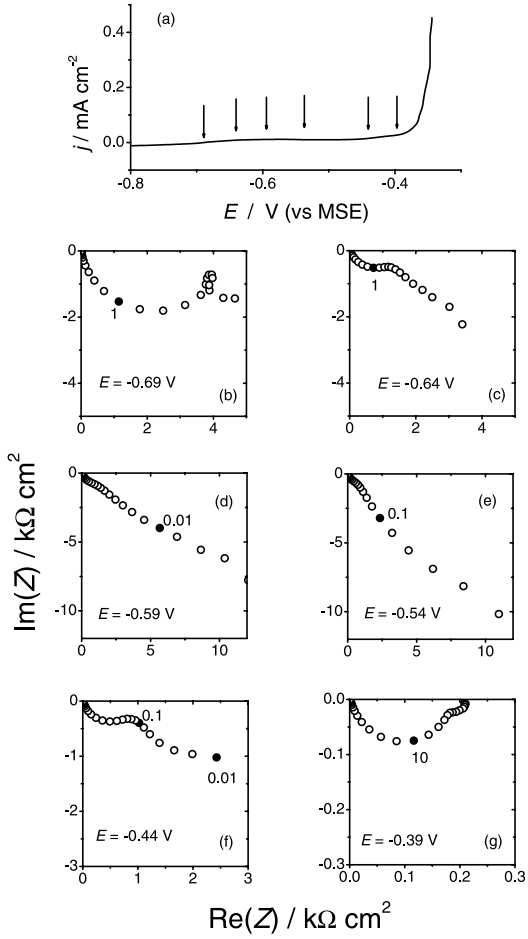

Fig. 6. Copper in aqueous 1 mM TU+0.5 M sulphuric acid. (a) Quasi-stationary polarisation curve recorded at $v = 0.0005$ V s^{-1}. (b–g) Impedance spectra at different E as indicated by the arrows in (a).

tical slope of 45°, is related to electrochemical reactions under diffusional control.

Under these circumstances, for comparable values of E, the Nyquist plots show that the former linear behaviour recorded at low frequencies now exhibits capacitive loops (compare Fig. 6c–d with Fig. 9b–c, for instance). Furthermore, as the increase in forced convection assists the transport of reacting species to the electrode surface, the impedance decreases markedly and at the same time the different contributions to the impedance are observed more clearly. Then, it can be concluded that in the range of the second time constant the corresponding electrochemical processes are influenced by hydrodynamic conditions irrespective of the frequency, as expected for mass transport kinetic control.

3.3.3. The transfer function

Experimental EIS data fit the following total transfer function:

$$Z_T(j\omega) = R_\Omega + Z(j\omega) \quad (1)$$

where $Z_T(j\omega)$ is the total transfer function; R_Ω, the electrolyte resistance contribution; $\omega = 2\pi f$, f, the frequency and $Z(j\omega)$ is the impedance of the interface that is specific of each electrochemical system. For copper either in aqueous 0.5 M sulphuric acid or in aqueous 0.1 mM TU+0.5 M sulphuric acid the expression of $Z(j\omega)$ is (Fig. 10a):

$$[Z(j\omega)]^{-1} = [Z_{CPE}]^{-1} + [R_{ct} + Z_w]^{-1} \quad (2)$$

where $Z_{CPE} = [C_{dl}(j\omega)^{\alpha}]^{-1}$ is the constant phase element; C_{dl}, the double layer capacitance; the exponent α accounts for the distribution of time constants due to surface inhomogeneities; R_{ct}, the charge transfer resistance defined as $R_{ct} = \lim_{\omega\to\infty} Re[Z]$ and Z_w is the impedance related either to diffusion through a film, of thickness d, formed on the electrode,

$$Z_w = R_{DO}(jS)^{-1/2} \tanh(jS)^{1/2} \quad (3)$$

or to diffusion from the solution when a 45° linear slope is observed,

$$Z_w = R_{DO}/(jS)^{-1/2} \quad (4)$$

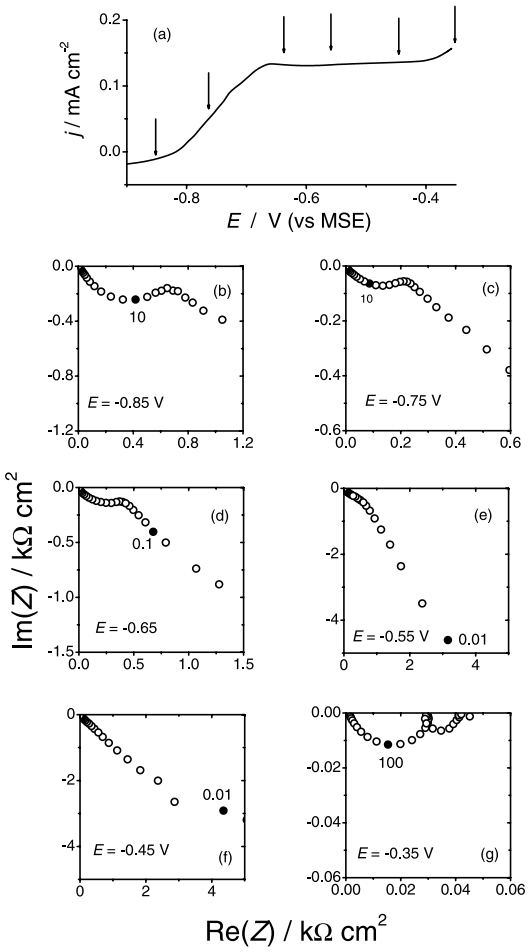

Fig. 7. Copper in aqueous 10 mM TU+0.5 M sulphuric acid. (a) Quasi-stationary polarisation curve recorded at $v = 0.0005$ V s^{-1}. (b–g) Impedance spectra at different E as indicated by the arrows in (a).

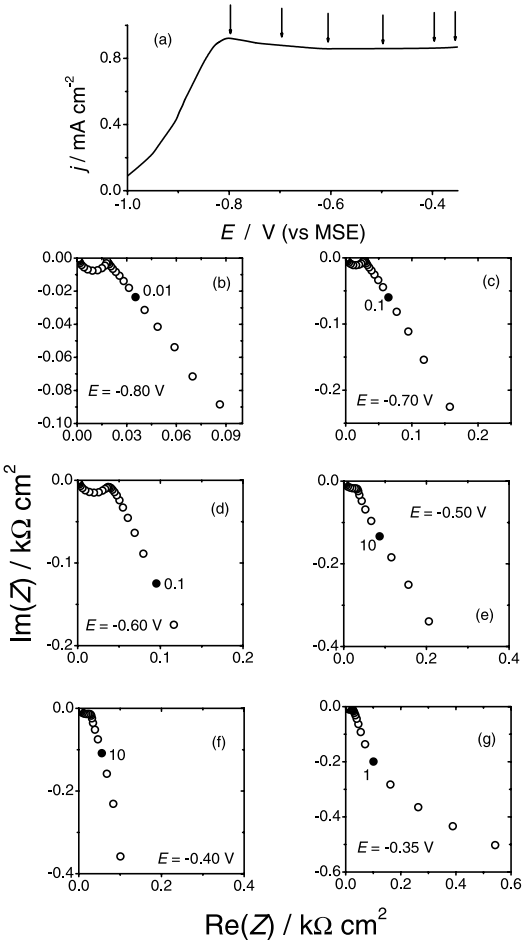

Fig. 8. Copper in aqueous 0.5 mM TU+0.5 M sulphuric acid. (a) Quasi-stationary polarisation curve recorded at $v = 0.0005$ V s^{-1}. (b–g) Impedance spectra at different E as indicated by the arrows in (a).

$R_{DO} = \lim_{\omega\to\infty} Z_w(j\omega)$ being the diffusion resistance for $\omega \to 0$ and $S = d^2/(\omega D)$, and D being the diffusion coefficient of species in solution.

Otherwise, for copper in aqueous 1 mM TU+0.5 M sulphuric acid and in aqueous 10 mM TU+0.5 M sulphuric acid the transfer function is described by (Fig. 10b):

$$[Z(j\omega)]^{-1} = [Z_{CPE}]^{-1} + \left[R_{ct} + \frac{R_1}{j\omega C_1 R_1 + 1} + Z_w\right]^{-1} \quad (5)$$

where R_1 and C_1 are related to a Faradaic pseudo-capacitive contribution of those electrochemical reactions involving adsorbates at intermediate frequencies.

Finally, for copper in aqueous 0.5 M TU+0.5 M sulphuric acid, the experimental data can be analysed using the transfer function (Fig. 10c):

$$[Z(j\omega)]^{-1} = [Z_{CPE}]^{-1} + [R_{ct} + Z_w]^{-1} + \frac{1}{j\omega C_L} \quad (6)$$

where C_L is the low frequency pseudo-capacitance related to the charge transport and accumulation process in the anodic film, i.e. a contribution usually denoted as 'finite length effects' [23].

Experimental data (Figs. 5–9), fitted according to Eq. (1) using conventional non-linear least-square fit routines, agree reasonably well (Fig. 11 and Table 1).

Values of the different parameters can be derived from the total transfer functions (Eqs. (2)–(6)). For copper in aqueous 0.5 M sulphuric acid from the first time constant it results in $C_{dl} \simeq 100$ μF cm^{-2}, $\alpha = 0.86 \pm 0.03$ and $R_{ct} \simeq 10\,000$ Ω cm^2. These figures remain practically constant irrespective of E. The high R_{ct} values indicate that in aqueous 0.5 M sulphuric acid copper dissolves very slowly. The value of D obtained from low frequency data is approximately 6×10^{-5} cm^2 s^{-1}, in good agreement with values reported in the literature [24].

For aqueous TU-containing 0.5 M sulphuric acid, the value of R_{ct} diminishes due to the fast electro-oxidation of TU that increases even with c_{TU}. For $c_{TU} = 0.5$ M, the lowest value of R_{ct} is reached, though its dependence on both c_{TU} and E is rather complex.

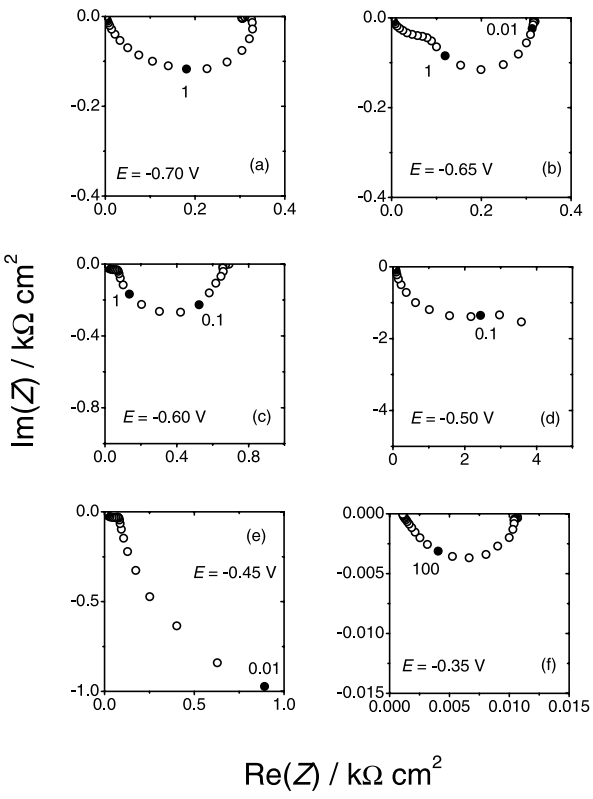

Fig. 9. Impedance spectra from copper rotating disk electrode in aqueous 1 mM TU+0.5 M sulphuric acid at different E. $\omega = 2000$ rpm.

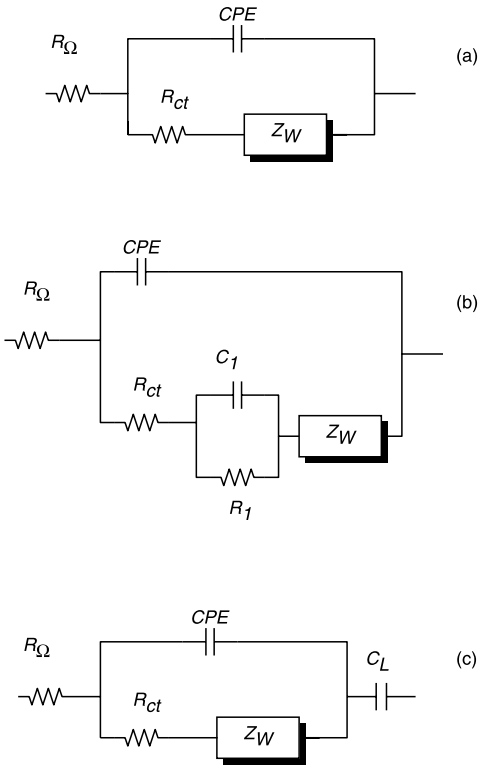

Fig. 10. Equivalent circuits corresponding to the transfer functions given by Eq. (2), (a); Eq. (5), (b) and Eq. (6), (c).

The values of the capacitance C for $c_{TU} \geq 1$ mM, are in the range 6–30 μF cm^{-2}, with $\alpha = 0.96 \pm 0.03$. These low values of C are typical of a metal covered by an insoluble film [25], and suggest that the metal | solution interface can be described as a set of two capacitances in series, so that $C^{-1} = C_{dl}^{-1} + C_{film}^{-1}$, where C_{dl} and C_{film} are related to the double layer and film capacitance, respectively. Accordingly, taking $C_{dl} \simeq 80$ μF cm^{-2}, the capacitance of the film results in 6–43 μF cm^{-2}.

On the other hand, the analysis of EIS data at intermediate frequencies becomes more complicated, because of the overlapping between the capacitive loops related to the first and the second time constants. Nevertheless, from fitted data, we estimate the range for C_1 values as $500 \leq C_1 \leq 800$ μF cm^{-2}. These values of C_1 are consistent with a pseudocapacitance related to TU electroadsorption on copper.

Finally, the inductive loop can be observed at intermediate frequencies at both high E and c_{TU} and they are related to copper pitting, as confirmed by SEM observations as described further on.

3.4. SEM micrographs

SEM micrographs from anodised copper electrodes were taken to confirm the formation of two distinct anodic films on copper, as concluded from EIS. The anodic film produced at high E in the presence of a large c_{TU} shows a strong capacitive response and its presence is bound to copper pitting corrosion. Pitting can explain the appearance of inductive loops in the Nyquist plots. For these purposes samples for SEM were prepared by anodising copper foils at $-0.4 \leq E \leq -0.35$ V for 120 min, in both aqueous 1 mM TU+0.5 M sulphuric acid and aqueous 0.5 M TU+0.5 M sulphuric acid.

Micrographs show two surface morphologies, principally depending on c_{TU}. For $E = -0.35$ V and $c_{TU} = 1$ mM, the anodic film exhibits a white appearance visible to the naked eye. SEM examination reveals its fibrous morphology (Fig. 12a–b) that is similar to that reported elsewhere for lower TU concentrations [19]. The EDAX analysis of this film confirms the presence of sulphur (Fig. 12c) its composition in atom% being in the range 35% S and 65% Cu–42% S and 58% Cu, depending on the surface region under observation. Note that though this atom ratio is close to the stoichiometry of Cu_2S, an enhanced contribution of the copper substrate should not be disregarded, a fact that could suggest to an overestimation of the percentage of copper in the sample. It should be noted that some pits whose chemical composition, according to EDAX examination, does not involve sulphur atoms are also observed (Fig. 13).

Copper foils anodised at $E = -0.4$ V in aqueous 0.5 M TU+0.5 M sulphuric acid produce a certain dull

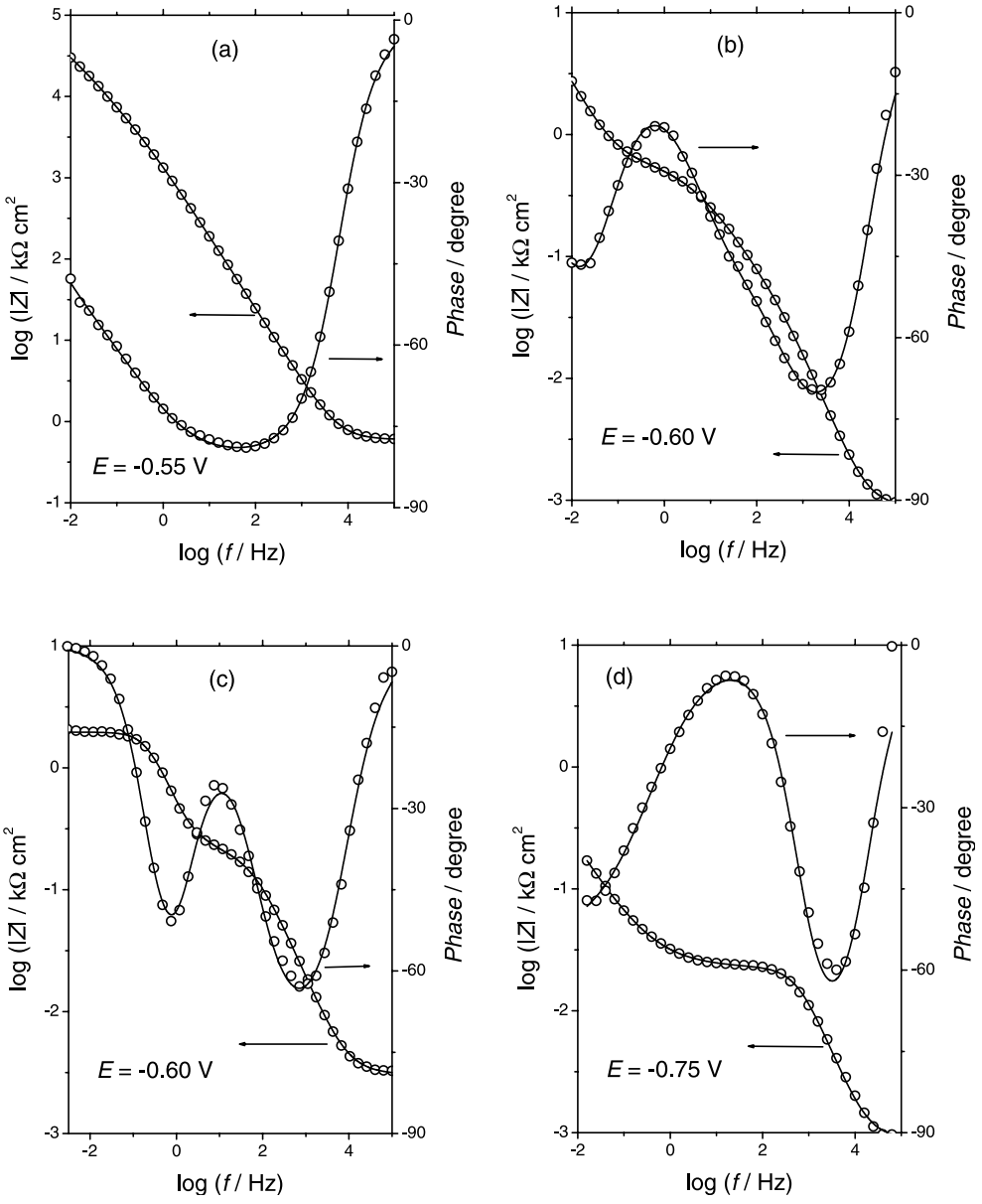

Fig. 11. Fitting of Bode plots for copper in aqueous 0.5 M sulphuric: (a) +0.1 mM TU, according to Eq. (2); (b) +10 mM TU, according to Eq. (5); (c) +1 mM TU, $\omega = 2000$ rpm, according to Eq. (5); (d) +0.5 M TU, according to Eq. (6). Parameters assembled in Table 1. (○) experimental data; (−) fitted data.

copper-like film. SEM micrographs show a smooth surface (Fig. 14a) with a film content of sulphur slightly higher than that of the anodic film described above, i.e. S 47%, Cu 53% (Fig. 14b). The film appears as quite compact in agreement with the Nyquist plots obtained for these experimental conditions which show a response

Table 1
Parameters used for fitting the experimental data shown in Fig. 11a–d

	R_Ω/Ω cm^2	C/μF cm^{-2}	α	R_{ct}/Ω cm^2	$10^{-3} \times Z_W$/Ω^{-1}	R_1/Ω cm^2	C_1/μF cm^{-2}	C_L/mF cm^{-2}
(a)	1.70	75.25	0.85	10.506	0.05	–	–	–
(b)	0.88	20.7	0.92	62.94	1.8	533.5	259	–
(c)	3.05	32.05	0.85	200	1.42	1391	513.3	–
(d)	0.91	21.6	0.93	22.02	2.5	–	–	26

close to that expected for a pure capacitor, i.e. there is diffusion impedance that tends to a vertical line due to the finite length effect [23] (Fig. 8).

4. Discussion

4.1. Reaction pathway framework

Previous electrochemical studies of the Cu | TU interface using conventional voltammetry, RDE and RRDE provided information about the likely reaction pathway and kinetics of the electrochemical reaction occurring there [11,19,21]. The observation of the electrode profiles by in situ transversal imaging [19] allowed us to determine some structural and kinetic characteristics of the anodic films formed in those processes. Likewise, STM and surface analysis of various metals in TU-containing solutions [12,13] have shown the formation of several self-assembled monolayers of adsorbates and their applied potential-dependent dynamics. From all these data, likely reaction pathways, particularly for the anodic processes, could be envisaged [11,21].

The reaction pathway related to the electrochemical reactions of TU and copper for $E > E_{oc}$ changes with E and c_{TU}. The first anodic reaction is the electro-oxidation of TU to FDS, a process, which is characterised well by a conjugated pair of voltammetric peaks (Fig. 2). The corresponding reactions behave as electrochemical processes under diffusion control that are somewhat interfered with by the presence of different adsorbates. These adsorbates likely include small amounts of sulphur produced by the slow decomposition of TU in the working solutions [26].

In any case, the electro-oxidation reactions at the Cu | TU-containing acid solution interface can roughly be described as three groups of reactions. At $E < -0.5$ V (range I) the electro-oxidation of TU to FDS is the main reaction. It involves the participation of TU adsorbates, the formation of soluble products, and for $E \rightarrow -0.4$ V, the appearance of minor amounts of sulphur-containing surface impurities.

At $-0.5 \leq E \leq -0.4$ V (range II), the electro-oxidation of TU to FDS is accompanied by copper electro-dissolution to Cu(I)–TU complexes. Among them for $c_{TU} \simeq 2.5$ mM, an insoluble Cu–TU complex film passivates the metal. As the concentration of TU is increased, the reaction range II shifts negatively and the dissolution of Cu(I)–TU complex is assisted as the formation of soluble Cu(I)–TU complexes is favoured. Reactions in ranges I and II approach quasi-stationary intermediate kinetics as demonstrated previously by means of RDE and RRDE techniques [21]. Film formation in range II appears as a diffusion controlled metal electro-dissolution taking place through the Cu(I)–TU complex insoluble film.

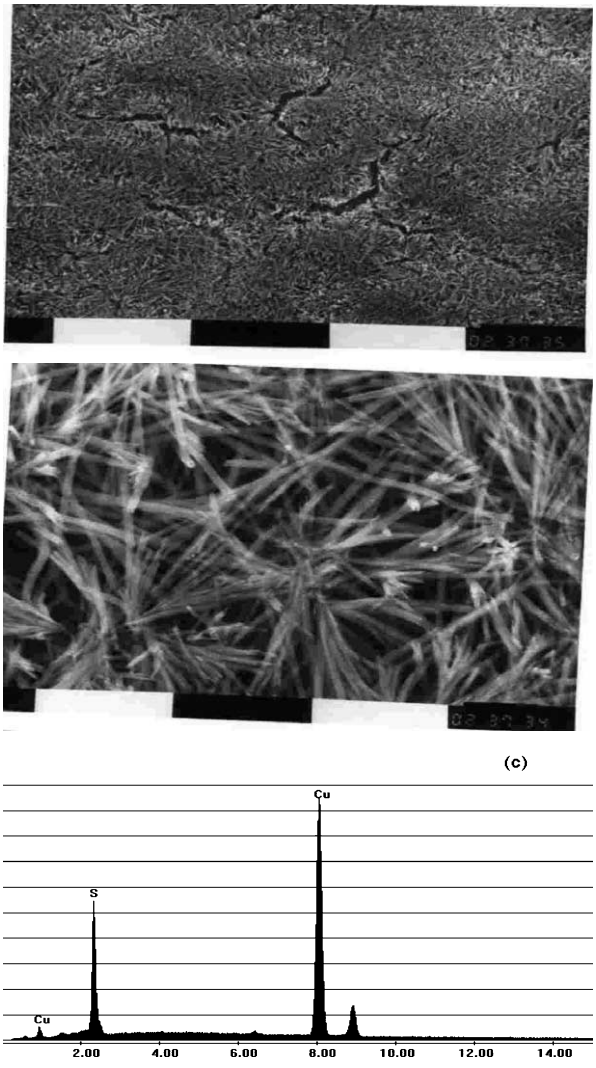

Fig. 12. SEM micrographs of a copper electrode anodised at −0.35 V for 120 min in aqueous 1 mM sulphuric acid. (a) Magnification 300 ×, scale 100 μm; (b) magnification 3000 ×, scale 10 μm; (c) EDAX spectrum.

At $E > -0.4$ V (range III), copper electrodissolution takes place. This reaction is accompanied by the partial electro-oxidation of Cu(I)–TU complexes yielding a passive sulphur-containing film as well as the formation of Cu(I)–TU complexes by the chemical reaction of Cu(II) with either TU or presumably FDS. These reactions tend to be dominated by localised processes producing copper pitting.

The above complex reaction pathway should be somewhat reflected by the behaviour of EIS of the entire system in the potential ranges I, II and III.

4.2. EIS in ranges I, II and III

For $E > E_{oc}$, transfer function interpretation of EIS can be made considering the preceding reaction pathway. In all cases, a first time constant at high frequen-

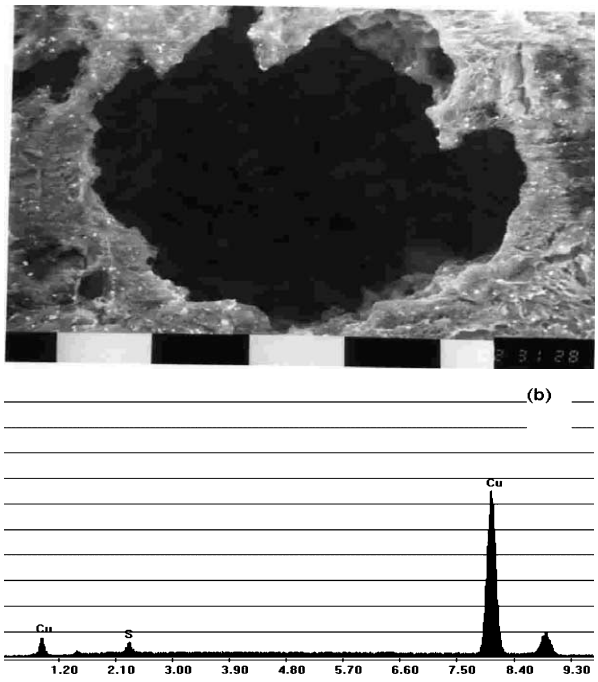

Fig. 13. (a) SEM micrograph of a crystallographic pit on a copper electrode anodised at −0.35 V for 120 min in aqueous 1 mM TU+0.5 M sulphuric acid. Magnification 2000×, scale, 10 μm; (b) EDAX spectrum.

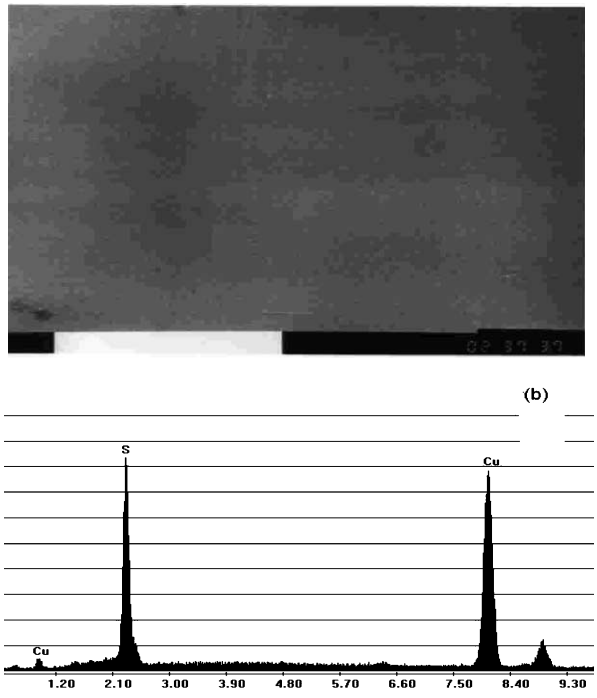

Fig. 14. (a) SEM micrograph of a copper electrode anodised at −0.4 V for 120 min in aqueous 0.5 M TU+0.5 M sulphuric acid. Magnification 500×, scale, 100 μm; (b) EDAX spectrum.

cies, due to a charge transfer reaction, and a second one in the low frequency range, due to diffusion transport are observed. The latter, depending on c_{TU} behaves as either a semi-infinite diffusion or a diffusion through an anodic film that was produced on copper. A third time constant, observed for $1 \leq c_{TU} \leq 10$ mM at intermediate frequencies, is related to a pseudocapacitive process and can be assigned to the electroadsorption of TU on copper. This process occurs in parallel with the charge transfer reaction related to the first time constant.

Let us first consider EIS of the Cu | TU interface for $0 \leq c_{TU} \leq 0.1$ mM (Figs. 4 and 5), involving two net time constants (Eq. (2)). For $c_{TU} = 0$, the value of the first time constant corresponds to a very slow reaction, presumably related to the electro-oxidation of water yielding copper oxide/hydroxide species at either a fractional monolayer or a few monolayer levels at E_{oc}. The rate of this reaction steadily increases as E approaches E_r^0(Cu(I)/Cu(II)). The second time constant is related to the diffusion of species produced by the electrodissolution of copper. In this case, the presence of two capacitive loops (Fig. 4a) has been explained by a reaction mechanism for copper electrodissolution that involves the formation of adsorbed Cu(I) species as precursors for the formation of aqueous Cu(II) ions diffusing into the bulk of the solution [24].

For $c_{TU} = 0.1$ mM (Fig. 5), the charge transfer resistance decreases considerably due to TU-assisted electrodissolution of copper yielding soluble Cu–TU complex species [21]. At $E < -0.7$ V this process is promoted by TU spontaneous adsorption on copper via the sulphur atom [27–31] producing a fractional monolayer coverage by deprotonated TU molecules, presumably through a partial charge transfer similar to that found for thiols [32]. The stoichiometry of these complexes depends on the TU concentration, as has been described elsewhere [14,21]. Their formation explains the second time constant at low frequencies that is related to the diffusion of soluble products to the bulk of the solution.

EIS obtained in the range $-0.6 \leq E \leq -0.5$ V is related to the formation of FDS from either an adsorbed intermediate [21] or a soluble radical ion [21,33]. The second time constant related to a Warburg-type impedance can be assigned to the diffusion of aqueous FDS from the bulk of the solution. Otherwise, for $E > -0.5$ V, the characteristics of diffusion changes from semi-infinite diffusion in solution to diffusion through a film. The latter happens when an anodic sulphide-containing layer from the electro-oxidation of soluble products is built. Then, the electro-oxidation reaction is determined by a transport of matter through the anodic film. As E approaches E_r^0(Cu(0)/Cu(II)), the rupture of the anodic film takes place. Accordingly, EIS shows inductive loops (Figs. 4 and 7) related to copper corrosion yielding soluble Cu(II) ions. In this case, the formation of soluble Cu(I) complex species can be controlled by the concentration of TU available at the

reaction interface for the homogeneous chemical reaction between Cu(II) ions and TU [8,34].

For $c_{TU} = 0.1$ mM, EIS resembles that found for copper in aqueous 0.5 M sulphuric acid (Figs. 4 and 5), in agreement with the low efficiency of TU as an inhibitor for copper corrosion at this c_{TU} [11,19].

For $1 \leq c_{TU} \leq 10$ mM, EIS involves three time constants (Eq. (5)). The first one represents again the charge transfer rate for the electro-oxidation of TU to FDS, i.e. the main electrochemical reaction for $E < -0.4$ V. The second time constant, which in part overlaps the frequency range of the first one and particularly its induction time related to the second time constant, confirms the pseudocapacitive process already referred to above. The corresponding adsorbates may be considered as precursors for anodic film formation at higher E. In fact, it has been reported [21] that, particularly for $c_{TU} \simeq c_{TU,c}$, the electro-oxidation of TU on copper is progressively hindered due to a gradual blockage of the copper surface by TU. For $E < -0.55$ V, the third time constant can be related to the outward diffusion of FDS, whereas for $E > -0.5$ V, the electrochemical process is controlled by diffusion through the anodic insoluble Cu–TU complex (Fig. 6e–f) and copper sulphide film, produced mainly from adsorbate electro-oxidation. In any case, the transport of reactants through the film, either Cu(I), Cu(II) outwards or TU inwards may control the anodic reaction at the copper surface [19].

The formation of an anodic sulphur-containing film, as concluded from SEM micrographs (Fig. 12), has an influence on the overall process that is observed by the current/potential response of the rotating ring disk experiments (Fig. 3). In this case, the appearance of the anodic film partially inhibits the electrodissolution of copper and its disappearance produces the reverse effects (Fig. 3). Correspondingly, EIS shows neither the inductive loops (Fig. 6), as for TU-free solutions (Fig. 4), nor Warburg-type contribution in the absence of kinetic control by the transport of soluble species. Then, the diffusional impedance is exclusively due to the diffusion of species through the anodic film (Fig. 9).

For $c_{TU} = 10$ mM, the polarisation curve shows a diffusion limiting current and an inhibition of copper electrodissolution at approximately -0.4 V. However, EIS is almost similar to that obtained for $c_{TU} = 1$ mM, although for $c_{TU} = 10$ mM the charge transfer resistance for the electro-oxidation of TU to FDS is smaller i.e. the electrode reaction is faster. Then, in agreement with the limiting anodic current observed in the polarisation curve, an outstanding Warburg-type contribution is found over a wider range of potential (compare Figs. 6 and 7). Likewise, the pseudocapacitive contribution is likely enhanced by the formation of soluble Cu(I)–TU complexes which assists either the electrodissolution of copper or the formation of the compact anodic film at $E > -0.45$ V. The thickness of the latter will depend on the competition between film growth and film dissolution reactions [19]. Therefore, for $c_{TU} = 10$ mM EIS shows an enhanced contribution of the diffusion through this film (Fig. 7f).

Finally, for $c_{TU} = 0.5$ M, the polarisation curve shows an anodic limiting current starting from $E \simeq -0.75$ V that is related to the electro-oxidation of TU to FDS and the electrodissolution of copper yielding soluble complex species such as $[Cu_2(TU)_6]^{2+}_{sol}$ [14,18]. The salt of this complex ion ($[Cu_2(TU)_6](SO_4)\cdot H_2O$) has been prepared by the electrochemical dissolution of copper in acid solutions at high c_{TU}, and characterised as a Cu(I) tetranuclear ion, $[Cu_4(TU)_{12}]^{4+}$, sited on a crystallographic inversion centre with all copper ions in a tetrahedral coordination with TU ligands and located at alternate sites on an eight-membered, crown-like ring [14]. It should be noted that at this high c_{TU} the insoluble film appears as a sticky insoluble complex. For $E \simeq -0.45$ V, the thickness and compactness of the film increase in such a way that the interface tends to behave as a pure capacitor (Fig. 8f), i.e. the electrical properties of the film dominate EIS. For such a film, EDAX analysis indicates that its inner part contains a greater amount of sulphur than that of films resulting from $c_{TU} = 1$ mM. It is noted that the lower percentage of sulphur found for the fibrous films might result from the open structure leaving large fractions of almost film-free copper, enhancing the contribution from the substrate. Furthermore, the voltammetric peak Ic related to the electroreduction of FDS to TU is no longer observed (Fig. 2d), in agreement with the presence of a compact film on copper acting as a barrier preventing the access of FDS molecules to the copper surface. For $E > -0.40$ V (Fig. 8g), EIS changes from a quasi-pure capacitor to that expected for diffusion through a film. In this case, the simultaneous electro-oxidation of FDS and Cu(I)–TU complexes, along with the electrodissolution of copper to aqueous Cu(II) ions takes place. Correspondingly, the nature and electrical characteristics of the anodic film change from a predominantly insoluble Cu(I)–TU complex film to a heterogeneous layered film consisting of copper sulphide and copper sludge [35]. The partial rupture of the copper sulphide-containing film leads to pitting corrosion. The formation of etched pits induced by sulphide contaminants from different environments has been extensively investigated [36–38]. The high rate of copper electrodissolution in 0.5 M TU at $E \simeq -0.3$ V results in a drastic thinning of the copper electrode and the pseudocapacitive contribution to EIS is no longer observed.

Let us consider now the values of the Warburg contribution at low frequencies, which for high c_{TU} is related to a finite length diffusion of TU through a film. Considering that for the fibrous open structured film (Fig. 12) its thickness is in the range $20 \leq d \leq 100$ nm, as reported from in situ-transversal imaging observa-

tions[19], the value of D then results in the range 10^{-6}–10^{-7} cm^2 s^{-1}, as expected for such a system.

On the other hand, the thickness of the compact film (Fig. 14) formed for $c_{TU} = 0.5$ M can be estimated considering that in this case $D = d^2/3C_L R$. Then, considering $D \simeq 10^{-10}$ cm^2 s^{-1}, as previously reported for films of similar characteristics [39,40], and that $40 \leq C_L \leq 260$ mF cm^{-2}, as results from the Nyquist plots, values of d in the range of $200 \leq d \leq 700$ nm are obtained.

5. Conclusions

- EIS of copper in aqueous TU-containing sulphuric acid obtained by stepping the potential in the range $-0.8 \leq E \leq -0.3$ V (vs. MSE), at different concentrations of TU in the range $0 \leq c_{TU} \leq 0.5$ M, provides new information about the complex electrochemical reactions related to TU and its byproducts, and to copper electrodissolution.
- The global transfer function that accounts for the behaviour of the Cu | TU solution interface depends on c_{TU}, E and hydrodynamic conditions. For $c_{TU} < 1$ mM, EIS data can be fitted considering a charge transfer resistance that dominates at high frequencies, coupled to a Warburg-type contribution that predominates at low frequencies. As c_{TU} is increased in the range $1 \leq c_{TU} \leq 10$ mM, three time constants are required for data fitting. The first one can be associated with TU electro-oxidation to FDS; the second one with a pseudocapacitive process predominantly related to TU electroadsorption on copper and the third one with a diffusional process in the presence of insoluble Cu(I)–TU complex anodic films.
- Depending on c_{TU}, when $E > -0.4$ V, either a fibrous type or a uniform, compact film is formed during the anodisation process.
- For $c_{TU} \geq 1$ mM the diffusional contribution depends on E. At low E it is related to diffusion in solution, whereas at high E it most likely corresponds to a Cu(I) transport through a compact anodic film.
- For $c_{TU} = 0.5$ M, the typical response of a pure capacitor is observed. This behaviour is explained by the formation of a film of uniform thickness, its conductivity increasing as E reaches a value close to the reversible Cu(0)/Cu(II) electrode potential. Then the formation of copper sludge in the film from the disproportionation of the Cu(I) species occurs.
- For either $c_{TU} \geq 1$ mM or $E > -0.4$ V the rupture of the anodic film is accompanied by the localised corrosion of copper yielding crystallographic pits.
- The conclusions of EIS data at different E and c_{TU} are consistent with the reaction pathways that have been previously proposed for the anodisation of copper in aqueous TU-containing sulphuric acid solutions.

Acknowledgements

This work was supported financially by the Consejo Nacional de Investigaciones Científicas y Técnicas (CONICET), Agencia Nacional de Promoción Científica y Tecnológica of Argentina (PICT 98 06-03251) and the Comisión de Investigaciones Científicas de la Provincia de Buenos Aires (CIC). J.N.L. thanks the Third World Academy of Science (TWAS) and CONICET for a fellowship granted.

References

[1] A. Szymaszek, J. Biernat, L. Pajdowski, Electrochim. Acta 22 (1977) 359.
[2] K.C. Pillai, R. Narayan, J. Electrochem. Soc. 125 (1978) 1393.
[3] T. Groenewald, J. Appl. Electrochem. 5 (1975) 71.
[4] M. Fleischmann, I.R. Hill, G. Sundholm, J. Electroanal. Chem. 157 (1983) 359.
[5] S. Méndez, G. Andreasen, P.L. Schilardi, M. Figueroa, L. Vázquez, R.C. Salvarezza, A.J. Arvia, Langmuir 14 (1998) 2515.
[6] L. Vázquez, R.C. Salvarezza, A.J. Arvia, Phys. Rev. Lett. 79 (1997) 709.
[7] P.L. Schilardi, O. Azzaroni, R.C. Salvarezza, A.J. Arvia, Phys. Rev. B59 (1999) 4638.
[8] P. Javet, H.E. Hintermann, Electrochim. Acta 14 (1969) 527.
[9] U. Bertocci, D.R. Turner, in: A.J. Bard (Ed.), Encyclopedia of Electrochemistry of the Elements, vol. II, Marcel Dekker, New York, 1974.
[10] G.V. Korshin, A.A. Petukhov, A.M. Kuznetsov, Y.M. Vyzhimov, Elektrokhimiya 27 (1991) 275.
[11] A.E. Bolzán, A.S.M.A. Haseeb, P.L. Schilardi, R.C.V. Piatti, R.C. Salvarezza, A.J. Arvia, J. Electroanal. Chem. 500 (2001) 533.
[12] O. Azzaroni, B. Blum, R.C. Salvarezza, A.J. Arvia, J. Phys. Chem. B 104 (2000) 1395.
[13] V. Brunetti, B. Blum, R.C. Salvarezza, A.J. Arvia, P.L. Schilardi, A. Cuesta, J.E. Gayone, G. Zampieri, J. Phys. Chem., in press.
[14] O.E. Piro, R.C.V. Piatti, A.E. Bolzán, R.C. Salvarezza, A.J. Arvia, Acta Crystallogr. B56 (2000) 993.
[15] M. Alodan, W. Smyrl, Electrochim. Acta 44 (1998) 299.
[16] F. Hanic, E. Durcanská, Inorg. Chim. Acta 3 (1969) 293.
[17] M.B. Ferrari, G.F. Gasparri, Crystallogr. Struct. 5 (1976) 935.
[18] R.C. Bott, G.A. Bowmaker, C.A. Davis, G.A. Hope, B.E. Jones, Inorg. Chem. 37 (1998) 651.
[19] A.S.M.A. Haseeb, P.L. Schilardi, R.C.V. Piatti, A.E. Bolzán, R.C. Salvarezza, A.J. Arvia, J. Electroanal. Chem. 500 (2001) 543.
[20] E.E. Reid, Organic Chemistry of Bivalent Sulfur, vol. 5, Chemical Publishing Co, 1963.
[21] A.E. Bolzán, I.B. Wakenge, R.C.V. Piatti, R.C. Salvarezza, A.J. Arvia, J. Electroanal. Chem. 501 (2001) 241.
[22] J.R. Macdonald, Impedance Spectroscopy, Wiley, New York, 1987.
[23] C. Ho, D. Raistrick, R.A. Huggins, J. Electrochem. Soc. 127 (1980) 343.
[24] D.K.Y. Wong, B.A.W. Coller, D.R. MacFarlane, Electrochim. Acta 38 (1993) 2121.
[25] A.M.P. Simões, M.G.S. Ferreira, B. Rondot, M. da Cunha Belo, J. Electrochem. Soc. 137 (1990) 82.

[26] M. Hoffmann, J.O. Edwards, Inorg. Chem. 16 (1977) 3333.
[27] A. Lukomska, S. Smolinski, J. Sobkowski, Electrochim. Acta 46 (2001) 3111.
[28] G. Horanyi, E.M. Rizmayer, P. Joó, J. Electroanal. Chem. 149 (1983) 221.
[29] D. Papapanayiotou, R.N. Nuzzo, R.C. Alkire, J. Electrochem. Soc. 145 (1998) 3366.
[30] G.M. Brown, G.A. Hope, D.P. Schweinsberg, P.M. Fredericks, J. Electroanal. Chem. 380 (1995) 161.
[31] G.M. Brown, G.A. Hope, J. Electroanal. Chem. 413 (1996) 153.
[32] D.W. Hatchett, K.J. Stevenson, W.B. Lacy, J.M. Harris, H.S. White, J. Am. Chem. Soc. 119 (1997) 6596.
[33] S.J.J. Reddy, V.N. Krishnan, J. Electroanal. Chem. 27 (1970) 473.
[34] H.M. Ratajczak, L. Pajdowski, Inorg. Nucl. Chem. 36 (1974) 431.
[35] S.H. Glarum, J.H. Marshall, J. Electrochem. Soc. 128 (1981) 968.
[36] T.P. Hoar, A.J.P. Tucker, J. Inst. Metals 81 (1952) 665.
[37] E.M. Kahiry, N.A. Darwish, Corros. Sci. 13 (1973) 141.
[38] D. Vázquez Moll, M.R.G. de Chialvo, R.C. Salvarezza, A.J. Arvia, Electrochim. Acta 30 (1985) 1011.
[39] R. Schrebler, H. Gómez, R. Córdova, L.M. Gassa, J.R. Vilche, Synth. Met. 93 (1998) 187.
[40] M.C. Montemayor, R. Jiménez, E. Fatás, J. Electroanal. Chem. 361 (1993) 115.